N63-13716
Code-1

NASA

TECHNICAL NOTE

D-1601

AERODYNAMIC DRAG AND STABILITY CHARACTERISTICS OF

TOWED INFLATABLE DECELERATORS AT SUPERSONIC SPEEDS

By John T. McShera, Jr.

Langley Research Center
Langley Station, Hampton, Va.

NATIONAL AERONAUTICS AND SPACE ADMINISTRATION

WASHINGTON   March 1963

NATIONAL AERONAUTICS AND SPACE ADMINISTRATION

TECHNICAL NOTE D-1601

AERODYNAMIC DRAG AND STABILITY CHARACTERISTICS OF

TOWED INFLATABLE DECELERATORS AT SUPERSONIC SPEEDS

By John T. McShera, Jr.

SUMMARY

/ 3 7/6

A wind-tunnel investigation has been conducted to study the possibility of inflating balloon and cone devices to give the same drag and stability characteristics as their solid counterparts over the Mach number range from 2.00 to 4.65. The results include some effects of Mach number, tow-cable length, and inlet configurations on the drag and stability of these inflatable decelerators.

Both the closed pressure-inflatable and self-inflatable (ram-air) decelerator configurations were fully inflated and had approximately the same drag and stability as their solid counterparts. The decelerator exhibits excellent stability in the supersonic wake region. The drag reaches a maximum and has little change with increases in tow-cable length when the decelerator reaches the supersonic wake region.

INTRODUCTION

The shortcomings of parachutes at high speed have been pointed out in references 1 and 2. Some of the stability inadequacies of low-porosity parachutes are discussed in these references and the drag levels of some high-porosity parachutes (stable configurations) are presented. These investigations have shown that parachutes having satisfactory operation exhibit relatively low drag coefficients at supersonic speeds.

In an effort to provide research data on decelerators, the National Aeronautics and Space Administration has made a continuing effort to investigate configurations which are both stable and produce high drag coefficients. References 3 and 4 show the results of tests made on configurations which have shown both high drag coefficients and stable operation in the tunnel. The models of reference 3 were exploratory in nature and were made of stiff plastic for which deformation under load was extremely low. The question then arises whether a satisfactory stowable decelerator can be designed which, when inflated, has adequate drag and stability characteristics.

This paper presents the results of an investigation to determine the adequacy of operation of some shapes previously tested and to measure the drag coefficients

of these models when they are constructed of inflatable materials. This paper shows some of the effects on drag and stable operation of tow-cable length. Also included are some results of inlet configurations on the operating characteristics of self-inflating configurations.

SYMBOLS

C_D	drag coefficient, F_D/qS
d	diameter of payload, 2.4 in.
F_D	force along wind axis, lb
l	tow-cable length, in.
M	Mach number
p	pressure, lb/sq ft
q	dynamic pressure, $0.7p_\infty M^2$, lb/sq ft
R	Reynolds number per ft
S	frontal area, sq ft

Subscripts:

t	total condition
∞	free-stream conditions
o	stagnation point
i	internal

APPARATUS

Wind Tunnel

The tests were conducted in the Langley Unitary Plan wind tunnel. The tunnel has two test sections of the variable-pressure return-flow type. The test sections are 4 feet square and approximately 7 feet in length. The nozzles leading to the test sections are of the asymmetric sliding-block type, and the Mach number may be varied continuously through a range from 1.5 to 2.8 in one test section and from 2.3 to 4.65 in the other. Further details of the wind tunnel may be found in reference 5.

2

Models and Instrumentation

A sketch of the test section and payload support system is shown in figure 1. The support system consisted of two thin struts which spanned the tunnel in the horizontal plane and which held the payload in the center of the tunnel. Throughout the tests only one payload was used and its shape was that of a cylinder, 2.4 inches in diameter and approximately 26 inches long.

Sketches of the closed pressure-inflatable models that were tested are shown in figure 2, and sketches of the ram-air or self-inflatable models tested are shown in figure 3. Figure 4 shows details of a typical front-inlet configuration and of a side-inlet configuration. Photographs of most of these models are shown in figure 5. The separation fence shown on these models is required for stability at subsonic speeds.

The models were attached with a 1/16-inch-steel tow cable to a drum which was mounted on an electrical strain-gage balance inside the payload. Use of the motor-driven drum gave the capability of changing the length of the tow cable without tunnel shutdown. A line tied from the back of the model to the main support system of the tunnel prevented the model from striking the test-section wall or from wrapping around the supporting strut during starting and shutdown of the tunnel. This line was kept slack during periods of the test when data were taken and had little, if any, effect on the data.

These models were fabricated from either nylon or Dacron cloth coated with neoprene. Typical schlieren photographs are presented in figure 6. In previous tests an attempt to scale the models dynamically was made; however, the models were not strong enough for the tunnel test conditions.

TESTS AND ACCURACY

The parameters for the configurations tested are shown in table I and are the ratio of length of tow cable to payload diameter l/d, the free-stream Mach number M_∞, the free-stream dynamic pressure q_∞, the Reynolds number R, the total tunnel pressure $p_{t,o}$, and the internal pressure p_i. The dewpoint temperature was maintained below -30° F to prevent adverse condensation effects. The stagnation temperature was maintained at 150° F for all Mach numbers except 2.00 and 4.65 where it was 125° F and 175° F, respectively.

The accuracy of the individual quantities is estimated to be within the following limits:

C_D . . . . ±0.02

l, in. . . . . ±0.5

$M_\infty < 3.95$ . . . . ±0.015

$M_\infty \gtrsim 3.95$ . . . . ±0.05

p_i, lb/sq ft . . . . ±2 percent

RESULTS AND DISCUSSION

The results of an investigation of several towed inflatable decelerators at Mach numbers from 2.00 to 4.65 are shown in figures 7 to 10. A motion-picture film supplement showing the 70° cone balloon as a closed pressure vessel and as a ram-air configuration has been prepared and is available on loan. A request card form and a description of the film will be found at the back of this paper, on the page immediately preceding the abstract page.

STABILITY

The motion picture shows the 70° cone balloon with and without side inlets. The side inlets fully inflate the model to the same shape as the closed pressure-inflatable 70° cone balloon. In comparison with parachutes tested under the same conditions, both these configurations and all the closed pressure-inflatable models discussed in this paper were very stable at the supersonic speeds investigated. The use of the word stability in this paper is taken as an indication of the absence of dynamic oscillations of the decelerator in the wind tunnel. Also shown in the movie is one of the earlier front-inlet ram-air configurations (an 80° cone balloon); this model never fully inflated and was extremely unstable. The movie shows the mass-flow pulsation phenomena which causes the vibratory fabric loading and subsequent failure that existed in many of the front-inlet ram-air cone balloons.

DRAG CHARACTERISTICS

Drag results for typical decelerator configurations at supersonic speeds are shown in figure 7. All of these configurations are simple in construction, are inherently stable at these speeds, and produce relatively high drag coefficients. This figure shows the effect of tow-cable length at various Mach numbers on the drag characteristics of a sphere, an 80° cone, and a 70° cone balloon. The 80° inflatable cone has approximately the same drag coefficient as its solid counterpart in reference 4. The 70° cone balloon has drag values that fall between those for the 60° and 80° solid cones. (See ref. 4.) Therefore, it appears that the cone balloon and the cone give similar if not identical results for a given cone angle. The sphere was not quite spherical in that it assumed a conical or pear shape due to its internal pressure. This shape had a cone apex angle of approximately 70°, therefore the data for the sphere are in close agreement with the 70° cone balloon.

It has been established in reference 4 that the stability of cones decreases with increasing cone angle, whereas the drag increases with increasing cone angle in the supersonic speed range, and that the cones with 90° apex angles were found to be intermittently unstable at the supersonic Mach numbers. Although no experimental results have been obtained, it appears that, based on the results of reference 4, an 80° cone balloon would be near optimum from the point of view of drag and stability. It was also pointed out in reference 4 that the wake from a payload at supersonic speeds can be divided into three regions - subsonic, transition, and supersonic. The dashed portion of the curves of figures 7 and 9 represent the extremities of the transition region, the range in which the flow field in front of the decelerator changes from subsonic to supersonic or vice versa. The arrows pointing upward represent the approximate point at which the flow field changed from subsonic to supersonic as the decelerator was being reeled out downstream, whereas the arrows pointing downward represent the approximate point at which the flow field changed from supersonic to subsonic as the decelerator was being pulled upstream towards the payload. The shape and location of this transition region are dependent on the ratio of the payload base diameter to decelerator diameter, the ratio of the tow-cable length to the payload diameter, the payload and decelerator shapes, the free-stream Mach number, and the flow field. The decelerator exhibits some degree of instability while passing through this transition region. In general, after passing this transition region, the stability of the decelerator becomes excellent and the drag coefficient reaches a maximum. Increases in l/d beyond maximum drag generally have little effect on the drag-coefficient level.

These inflatable decelerators have better drag and stability characteristics than parachutes, and yet they have approximately the same stowed density as parachutes. However, the use of inflatable decelerators requires that the system contain some device for maintaining its proper inflation pressure throughout its trajectory as the increased ambient pressure and increased dynamic pressure, depending on the velocity and altitude, demand an increased pressure requirement inside the system.

To avoid the problem of having heavy inflation equipment aboard the payload, the need for a self-inflating configuration was realized. The initial solution to this problem was to utilize the same technique as was used on a parachute; that is, to use the ram air (dynamic pressure) to inflate the decelerator to its initial shape and to maintain its inflation down to sea level, with the possibility of eliminating the requirement for deployment of a final-stage parachute. Many different means of inflating the 70° ram-air cone balloon were employed, most of them centered around front-inlet configurations. However, a mass-flow pulsation phenomena occurred in the supersonic speed range and resulted in vibratory fabric loading and subsequent failure of the models. As shown in figure 7, this problem did not appear in the closed pressure-inflatable models. It was found that this pulsation problem could be prevented by placing different porosity screens over the inlet and by using a cup to channel the air into the cone balloon. The variation of drag coefficient with tow-cable length for two typical configurations of this type is shown in figure 8. As can be seen, this arrangement lowered the drag value considerably as compared with the results for the closed pressure-inflatable models.

A side-inlet configuration of the 70° and 80° cone balloons was developed as a result of tests conducted at a Mach number of 10. (See ref. 6.) These results indicated that the wake from the payload did not tend to collapse or recover at any distance aft of the payload that could be tested within the tunnel (capability of the tunnel is $l/d = 18$). The entire diameter of the ram-air inlet was completely immersed in the core of this wake; therefore, the side inlets were used to feed the ram air into the cone balloon. This method of extended ram-air inlets worked very well at a Mach number of 10 (ref. 6) and at the supersonic speeds presented herein. (See fig. 9.) The side inlets on the 70° cone balloon fully inflated the model to the same shape as the closed pressure-inflatable 70° cone balloon, and the same drag coefficients were attained. However, lower drag coefficients were obtained with the 80° ram-air cone balloon having side inlets than with the 80° cone. This difference results from the fact that the cone balloon had a cup on the front similar to that shown in figures 4 and 5(c) and, therefore, that the cone balloon was closer in shape to a sphere than an 80° cone balloon.

A summary plot of the variation of the drag coefficients with Mach number of all the configurations tested is shown in figure 10. This figure represents data for $l/d = 8$, which in all cases is in the supersonic region of the wake. The 70° and 80° cone balloon with side inlets had internal pressures as high as 4 to 8 times dynamic pressure (table I). Previous tests indicate that a pressure equal to dynamic pressure was all that was needed to inflate the decelerator. The location of the side inlets may be changed in order to vary the amount of pressure inside the decelerator. Heating rates encountered on the inlets, however, may become severe, depending on the location of the side inlets.

CONCLUSIONS

The investigation of the drag and stability characteristics of towed inflatable decelerators at supersonic speeds has led to the following conclusions:

1. The closed pressure-inflatable models can be inflated to nearly the same shape as their solid counterpart, thereby giving the same drag and stability characteristics.

2. The ram-air or self-inflatable models with side inlets can be inflated in the wind tunnel, and, once inflated, they can maintain a design shape with changes in Mach number and dynamic pressure over the range tested.

3. In general, the decelerator exhibits high drag coefficients, and these coefficients level off at a maximum value which seems to be independent of tow-cable length after passing into the supersonic region of the wake.

6

4. In comparison with other drag devices, the inflatable decelerators, both closed pressure-inflatable and self-inflatable or ram air, were stable at the supersonic speeds investigated.

Langley Research Center,
    National Aeronautics and Space Administration,
        Langley Station, Hampton, Va., November 7, 1962.

REFERENCES

1. Maynard, Julian D.: Aerodynamics of Decelerators at Supersonic Speeds. Proc. of Recovery of Space Vehicles Symposium (Los Angeles, Calif.), Inst. Aero. Sci., Sept. 1960, pp. 48-54.

2. Maynard, Julian D.: Aerodynamic Characteristics of Parachutes at Mach Numbers From 1.6 to 3. NASA TN D-752, 1961.

3. McShera, John T., and Keyes, J. Wayne: Wind-Tunnel Investigation of a Balloon as a Towed Decelerator at Mach Numbers From 1.47 to 2.50. NASA TN D-919, 1961.

4. Charczenko, Nickolai, and McShera, John T.: Aerodynamic Characteristics of Towed Cones Used as Decelerators at Mach Numbers From 1.57 to 4.65. NASA TN D-994, 1961.

5. Anon.: Manual for Users of the Unitary Plan Wind Tunnel Facilities of the National Advisory Committee for Aeronautics. NACA, 1956.

6. Kayser, L. D.: Pressure Distribution, Heat Transfer, and Drag Tests on the Goodyear Ballute at Mach 10. AEDC-TDR-62-39 (Contract No. AF 40(600)-800 S/A 24(61-73)), Arnold Eng. Dev. Center, Mar. 1962.

TABLE I.- CONFIGURATIONS AND TEST CONDITIONS

Configuration	l/d range	M_∞	q_∞, lb/sq ft	R, per ft	$p_{t,o}$, lb/sq in.	p_i, lb/sq ft
80° cone (closed, pressure inflatable) 7-in. diam.	3.6 to 12.6	2.00	150	0.67×10^6	2.93	750
	1.6 to 13.0	2.50	150	.68	4.07	1,050
	1.6 to 12.6	2.87	150	.76	5.45	900
	1.0 to 12.2	3.50	125	.77	7.87	1,000
	1.1 to 8.00	4.65	150	1.30	23.97	990
Sphere (closed, pressure inflatable) 8-in. diam.	1.0 to 11.2	2.00	150	0.67×10^6	2.93	375
	0.5 to 11.9	2.50	150	.68	4.07	375
	1.1 to 11.4	2.87	150	.76	5.45	375
	1.7 to 9.0	3.50	125	.77	7.89	420
	1.1 to 9.0	3.96	150	1.09	13.66	420
70° cone balloon (closed, pressure inflatable) 7-in. diam.	0.7 to 12.1	2.00	150	0.67×10^6	2.93	375
	1.2 to 12.3	2.50	150	.68	4.07	450
	0.9 to 12.1	2.87	150	.76	5.45	450
	1.0 to 8.0	3.50	250	1.54	15.45	725
	1.0 to 8.0	3.96	250	1.82	22.76	725
	1.0 to 8.0	4.65	250	2.24	39.96	725
70° cone balloon (ram air, side inlets) 7-in. diam.	1.0 to 8.1	2.50	250	1.15×10^6	6.78	400
	0.5 to 8.5	3.50	250	1.54	15.45	475
	1.0 to 9.0	3.96	250	1.82	22.76	750 to 1,000
	1.0 to 9.0	4.65	250	2.24	39.96	400
80° cone balloon (ram air, front inlet) 8-in. diam.	4.0 to 8.0	2.50	150	0.68×10^6	4.07	200
	4.0 to 8.0	3.50	150	.79	9.27	200
80° cone balloon (ram air, side inlets) 8-in. diam.	2.0 to 9.0	2.50	250	1.15×10^6	6.78	2,100
	2.0 to 9.0	3.50	250	1.54	15.45	2,100
	2.0 to 9.0	3.96	250	1.82	22.76	2,100
	4.0 to 9.0	4.65	250	2.24	39.96	2,100
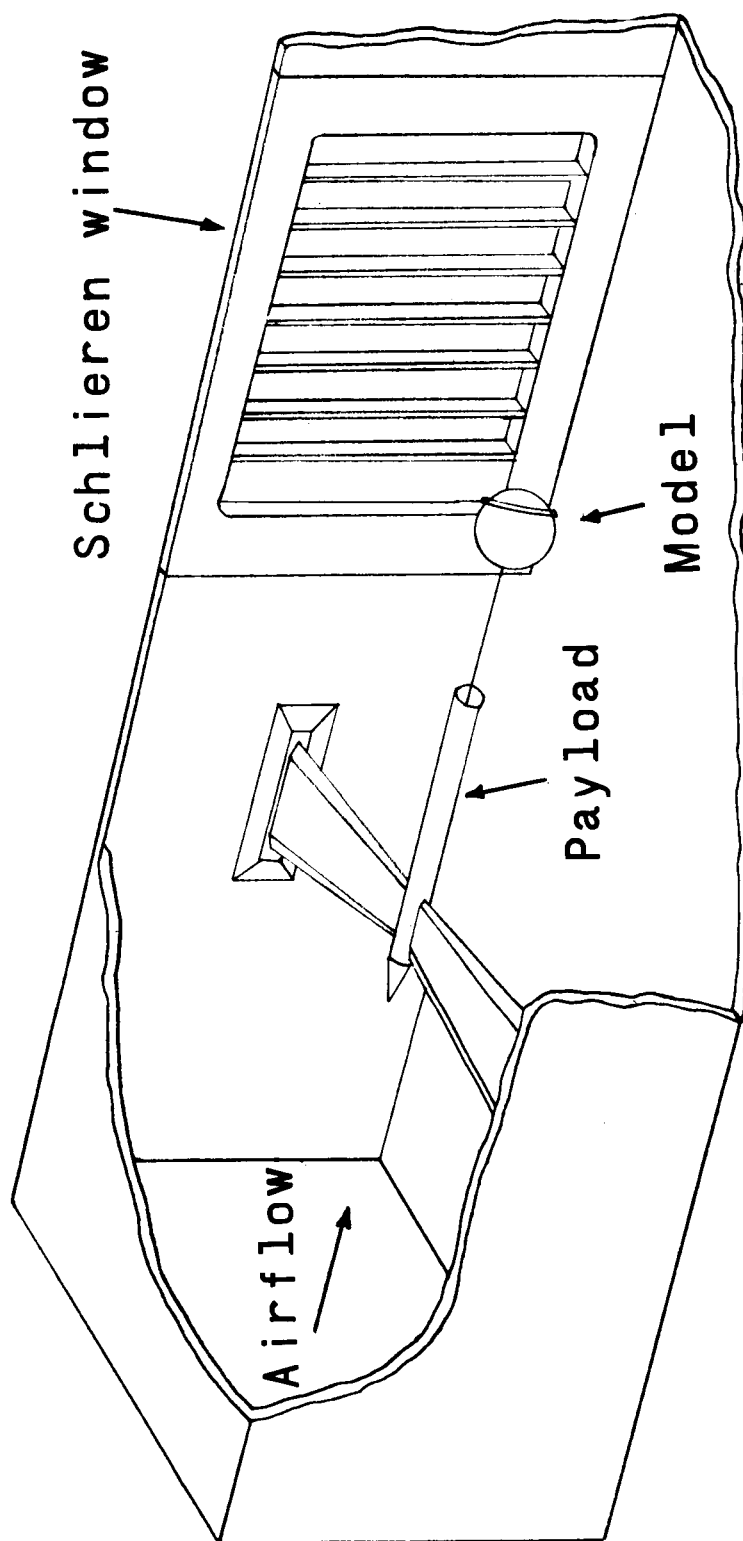
Figure 1.- Sketch of tunnel test section with payload and support system.
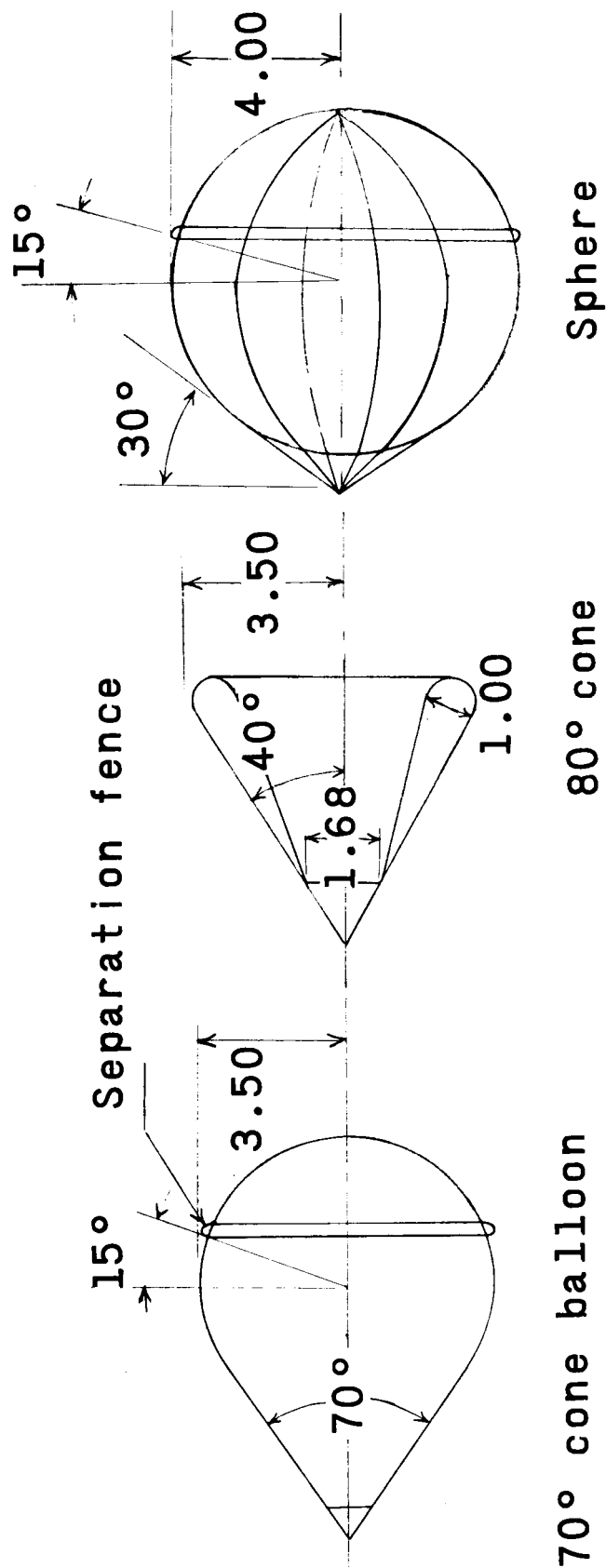
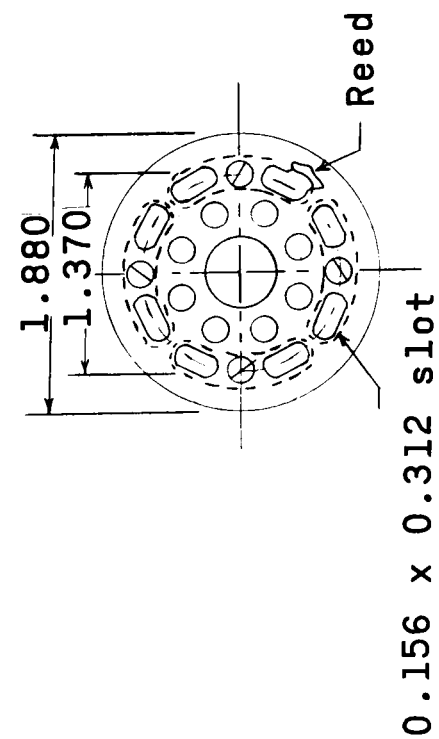Figure 2.- Drawing of closed pressure-inflatable models. (All dimensions are in inches unless otherwise noted.)

Separation fence

Meridian straps

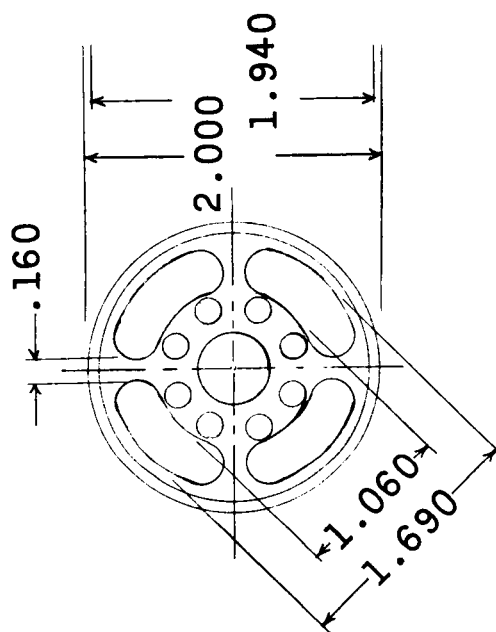4.00 40°

rear ring

nose ring
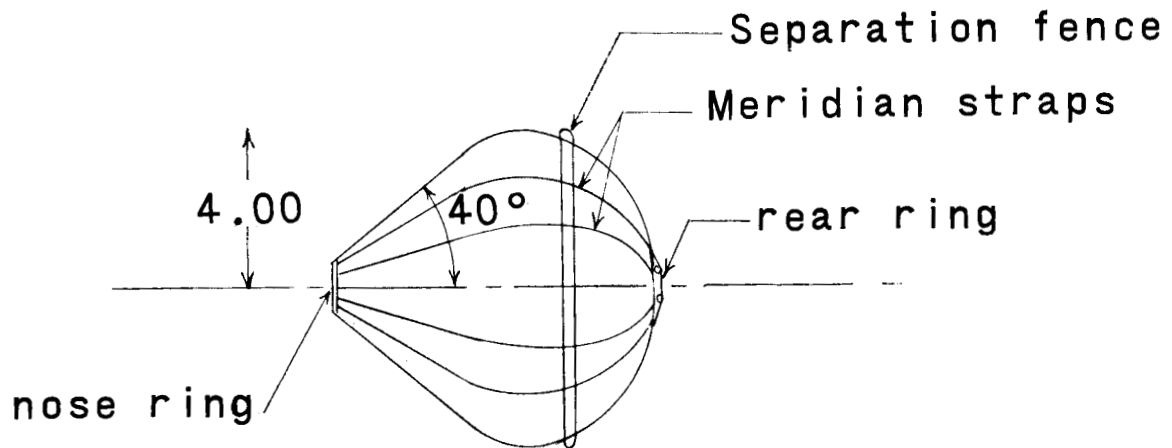
80° cone balloon with front inlet

0.50 0.37 4 side inlets
(equally spaced)

3.50 35° 11-percent-
porosity screen

Separation fence
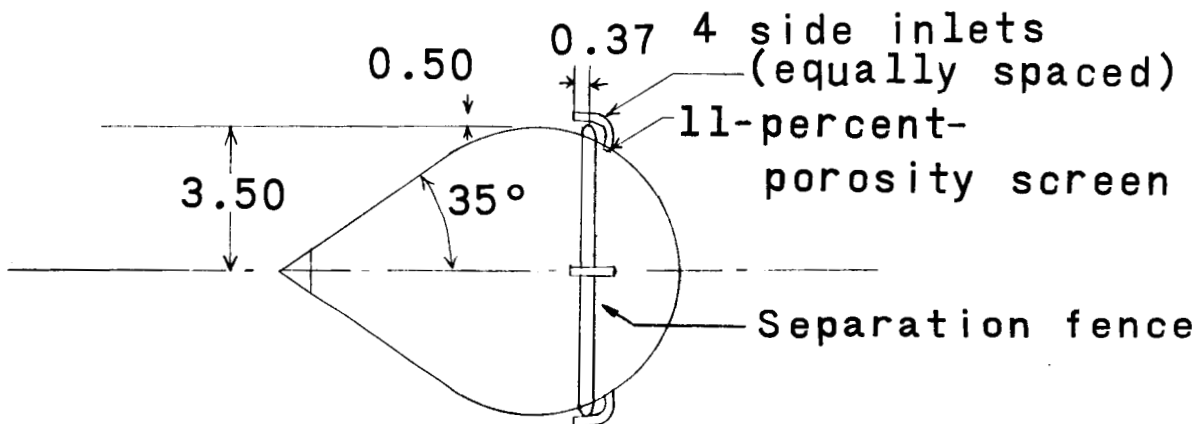
70° cone balloon with side inlets

Figure 3.- Drawing of self-inflatable (ram-air) models. (All dimensions are in inches unless otherwise noted.)

0.156 x 0.312 slot

Front inlet

Reed

Front-inlet cup

Side inlet (aluminum tube)

Wall thickness

Separation fence
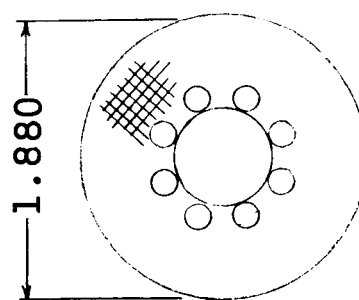
Screen

Front-inlet screen

Figure 4.- Details of front- and side-inlet configurations. (All dimensions are in inches.)
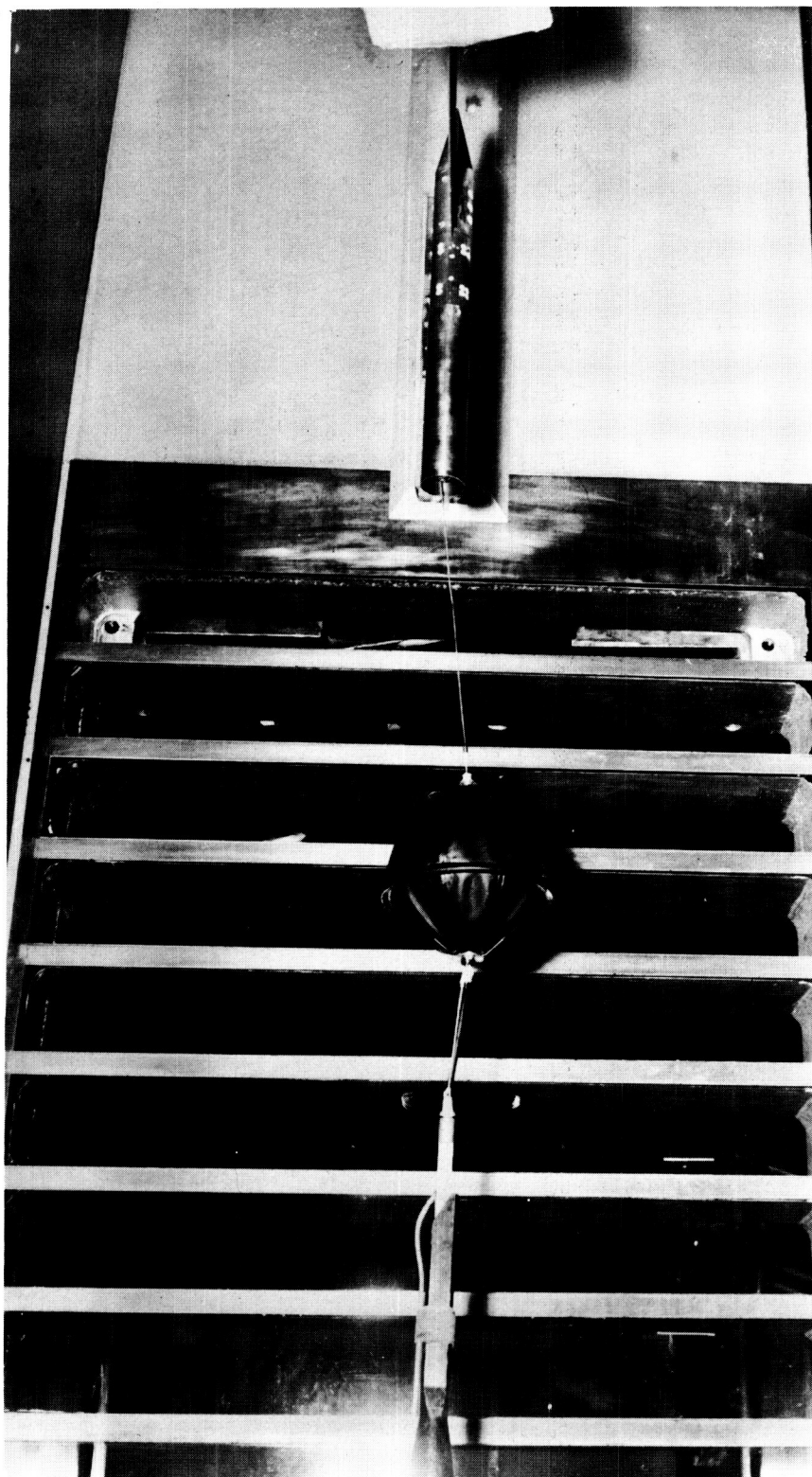
(a) Sphere.   L-62-5052

Figure 5.- Model photographs.

(b) 70° cone balloon.   L-62-3480

Figure 5.- Continued.

14
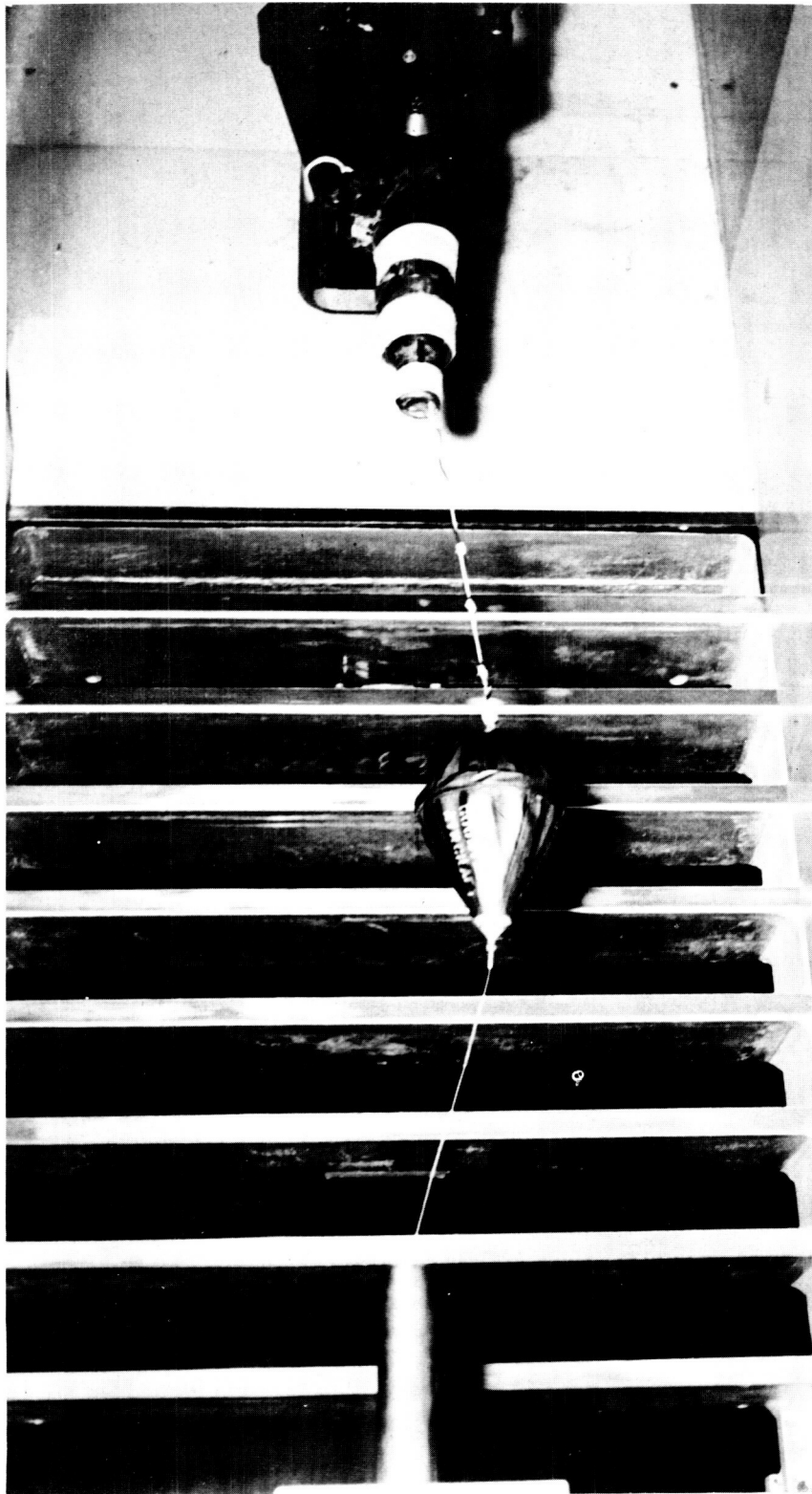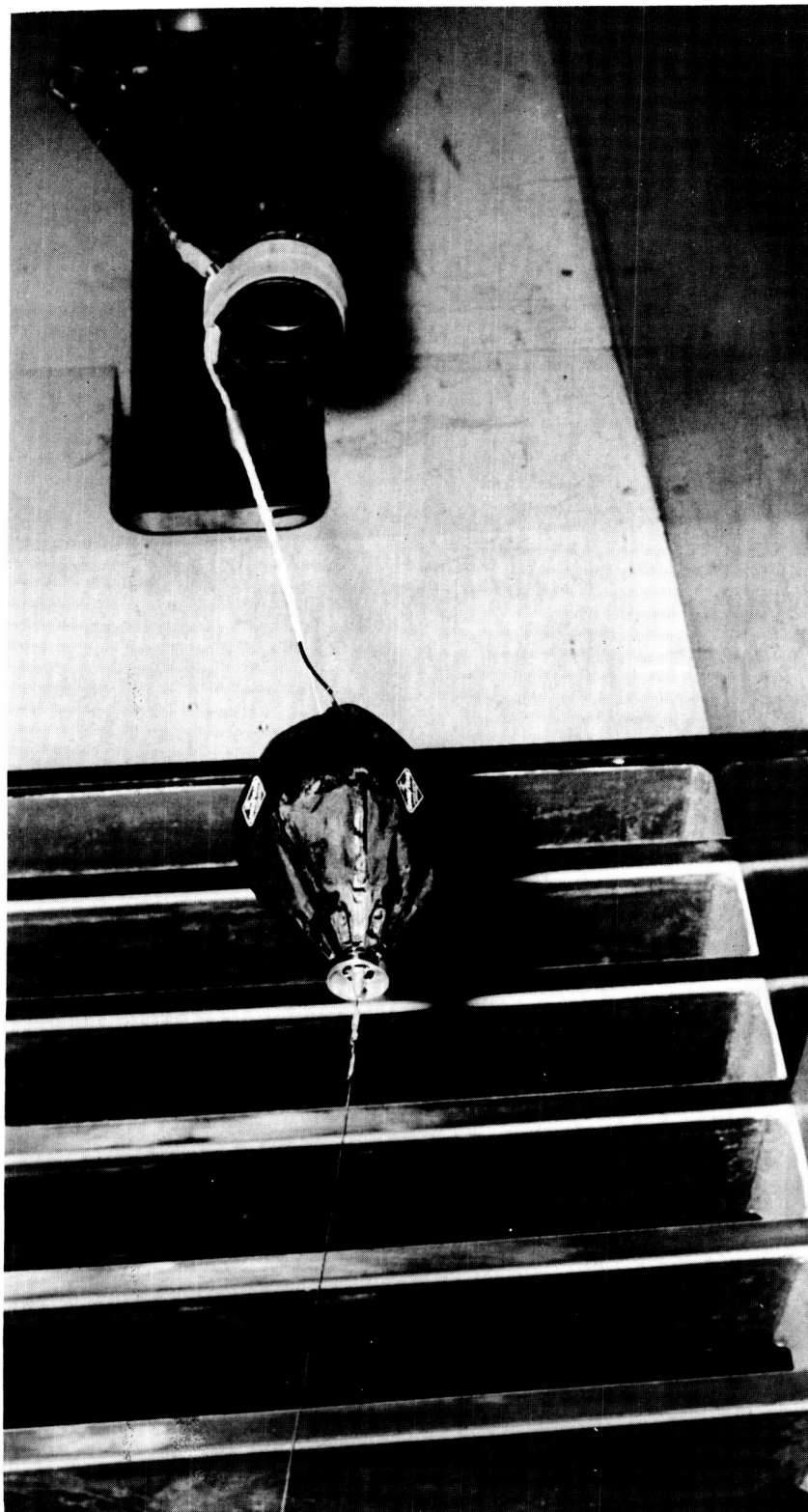
(c) 80° ram-air cone balloon with reed valve and cup.   L-61-4729

Figure 5.- Continued.
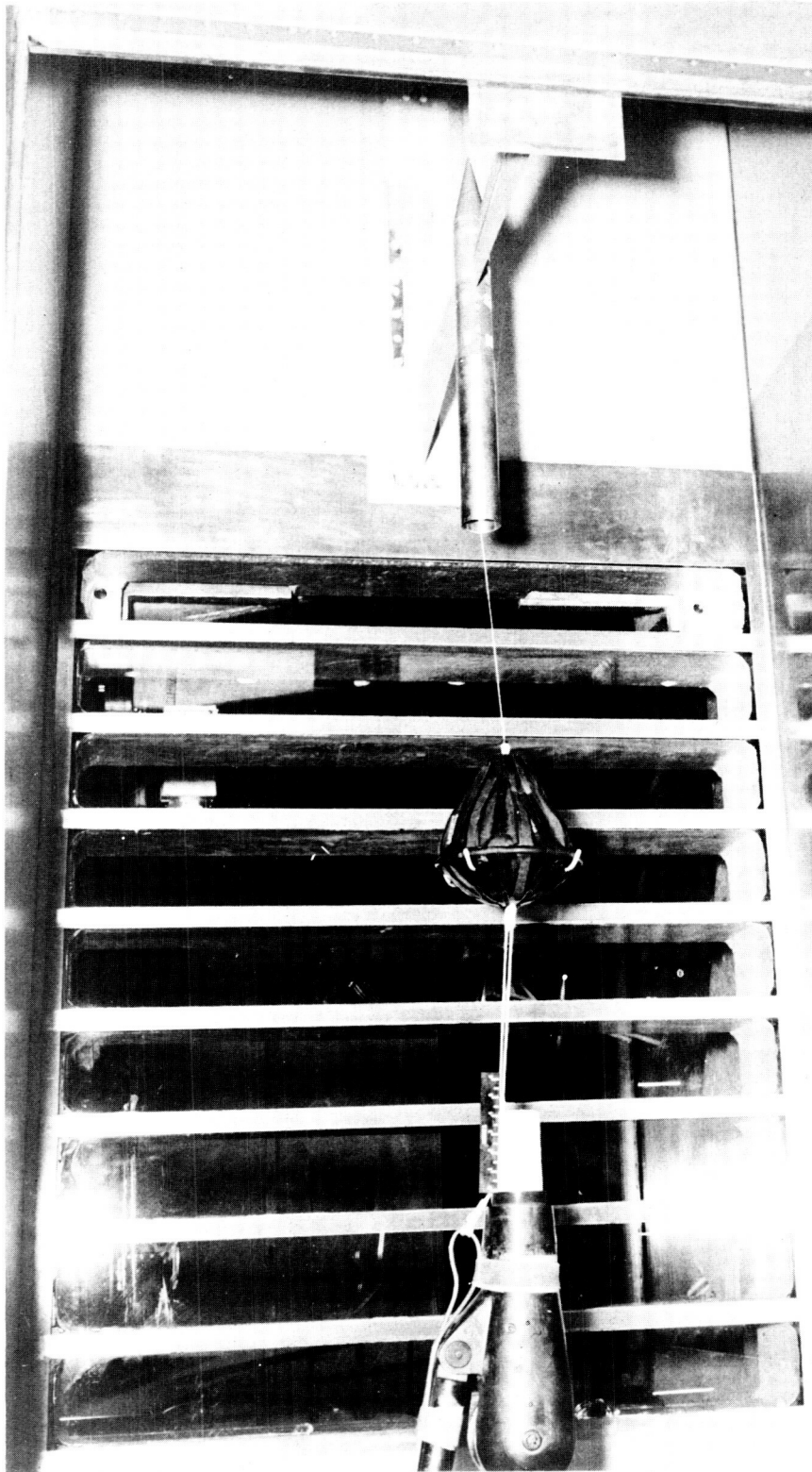
(d) 80° ram-air cone balloon with side inlets.   L-62-5085

Figure 5.- Concluded.

$l/d = 1.14$

$l/d = 2.26$

M = 3.96

$l/d = 4.42$

$l/d = 8.60$

Sphere

Figure 6.- Typical schlieren photographs.   L-62-7033

$M = 2.50$
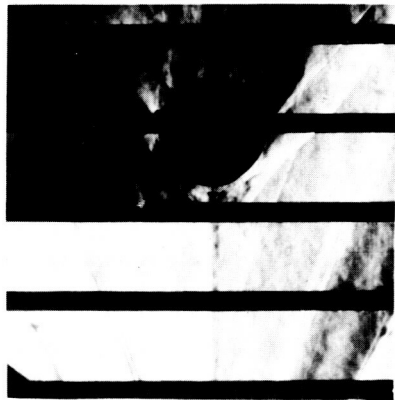
$l/d = 4.15$

$l/d = 6.98$

$l/d = 6.66$

$M = 3.50$

$l/d = 5.45$

$l/d = 9.79$

$l/d = 5.46$
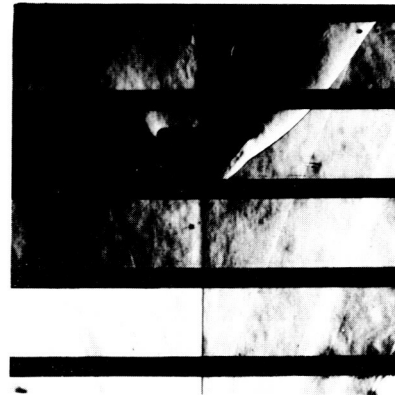
70° cone balloon with side inlet

80° cone

Sphere

Figure 6.- Concluded.   L-62-7034

18
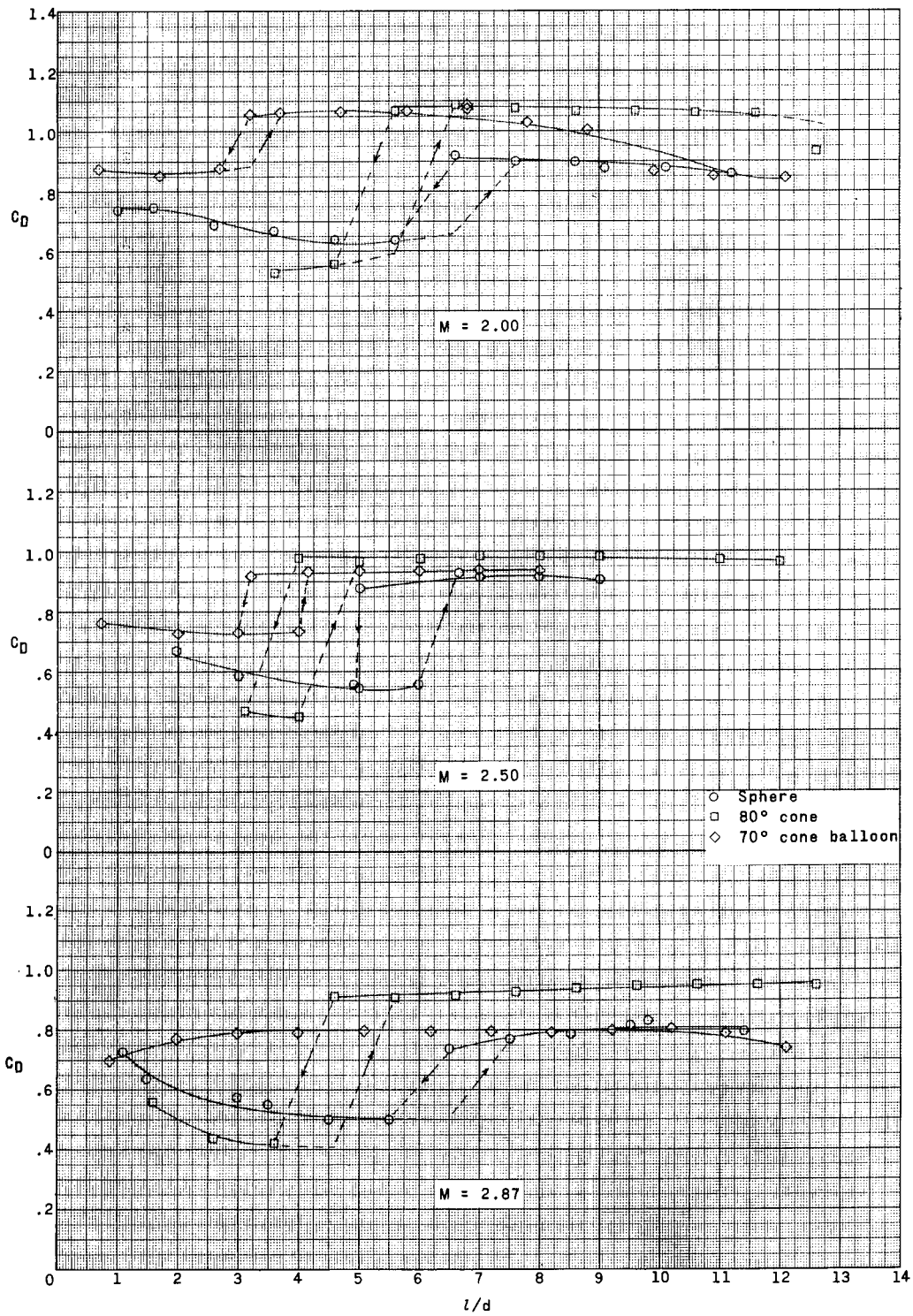
Figure 7.- Variation of drag coefficient with tow-cable length for closed pressure-inflatable configuration.
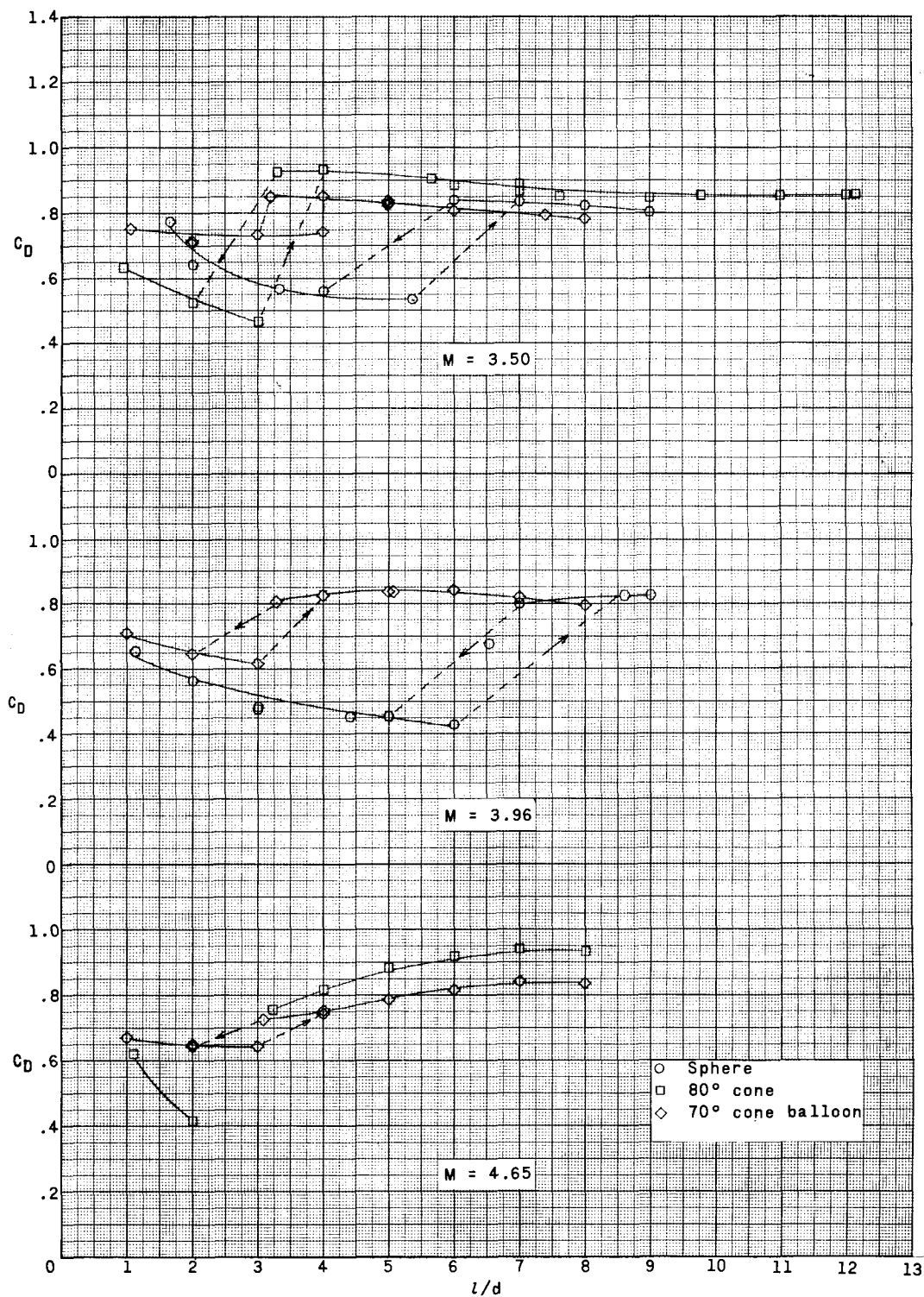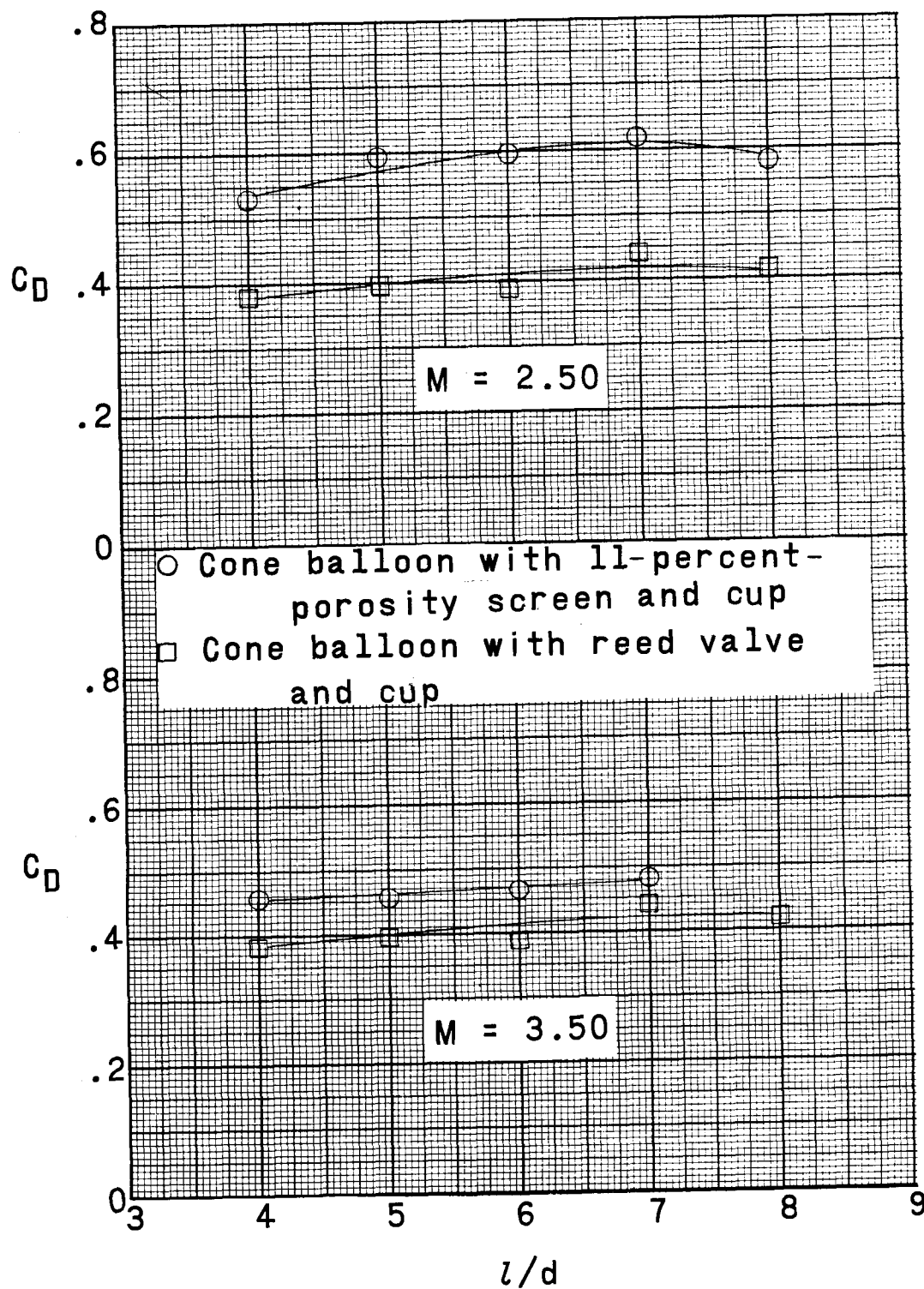
Figure 7.- Concluded.

Figure 8.- Variation of drag coefficient with tow-cable length for 80° ram-air or self-inflatable configuration.
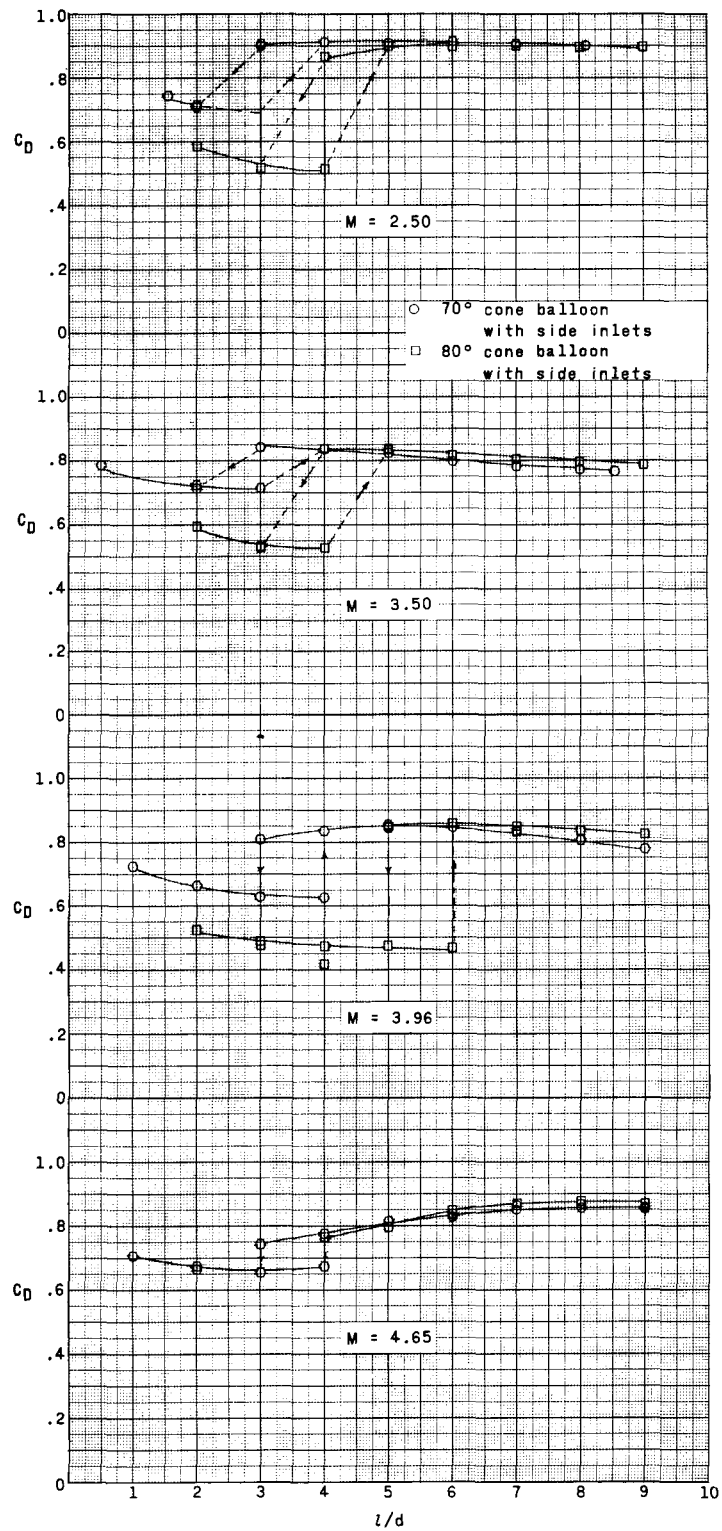
Figure 9.- Variation of drag coefficient with tow-cable length for two side-inlet configurations.
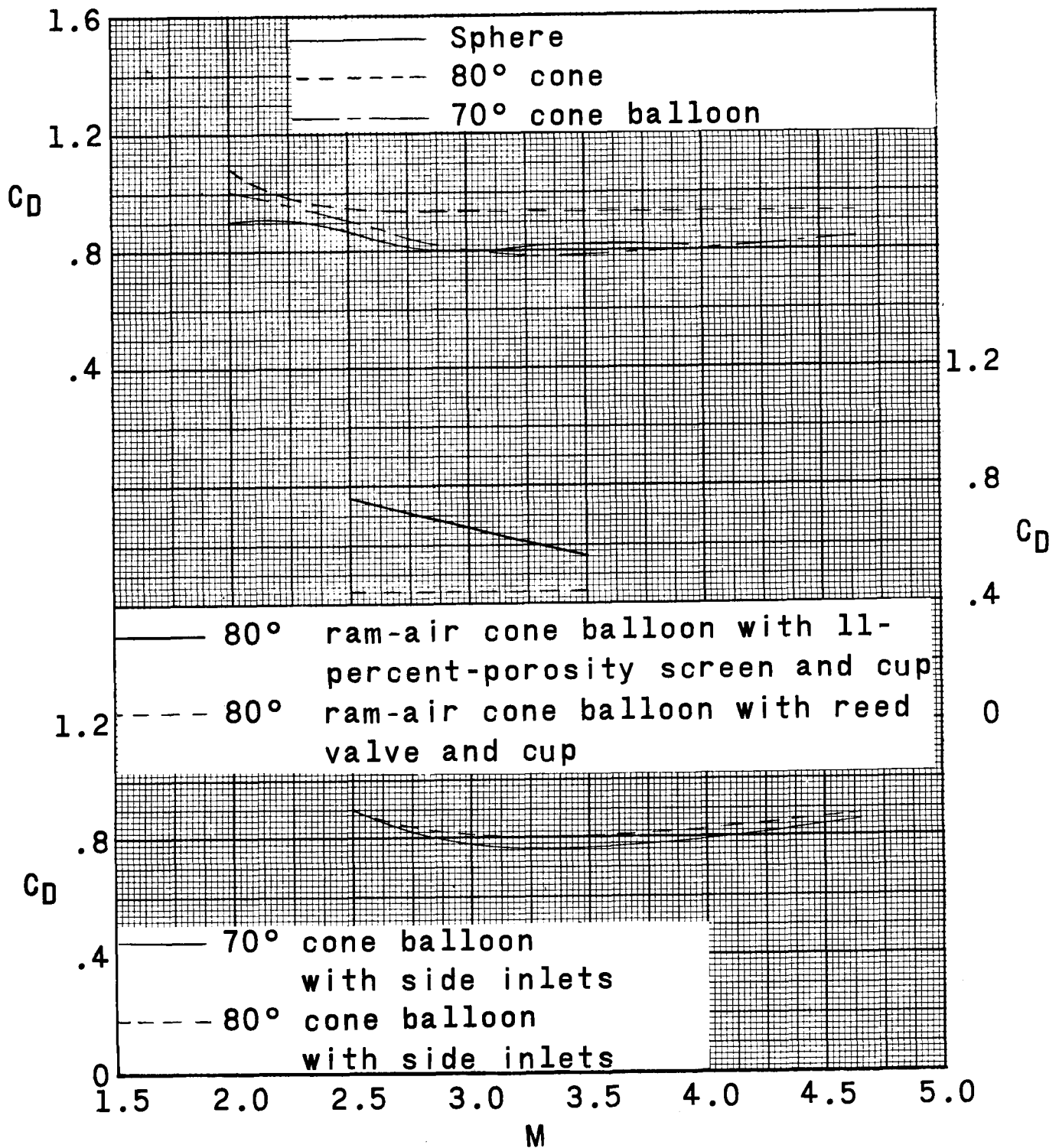
Figure 10.- Summary of drag coefficient plotted against Mach number for all configurations. $l/d = 8$.